Organic & Biomolecular Chemistry

Cite this: *Org. Biomol. Chem.*, 2012, **10**, 4891

www.rsc.org/obc

PAPER

Supramolecular polymerization of oligopyrenotides – stereochemical control by single, natural nucleotides†‡

Alina L. Nussbaumer, Florent Samain, Vladimir L. Malinovskii and Robert Häner*

Received 13th February 2012, Accepted 1st May 2012
DOI: 10.1039/c2ob25320h

Amphiphilic heptapyrenotides (Py_7) assemble into supramolecular polymers. Here we present a comprehensive spectroscopic study of aggregates and co-aggregates of the non-chiral Py_7 and its mono- or di-substituted nucleotide analogs (Py_7-N and N-Py_7-N′). The data show that the formation of supramolecular polymers from oligopyrenotides is highly sensitive to the nature of the attached, chiral auxiliary. A single natural nucleotide may be sufficient for the fine tuning of the aggregates' properties by changing the mechanism of aggregation from an isodesmic to a nucleation–elongation process, which results in a high degree of amplification of chirality in the formed supramolecular polymers. Watson–Crick complementarity does not play a significant role, since co-aggregates of oligomers modified with complementary nucleotides show no signs of supramolecular polymerization. Depending on the nucleotide, the helical sense of the polymers is shifted to an *M*-helix or a *P*-helix. The findings demonstrate the value of oligopyrenotides as oligomeric building blocks for the generation of optically active supramolecular polymers.

Introduction

Due to its self-assembling properties, DNA is one of the most prominent biological molecules used to build multidimensional nanostructures and nanomaterials.[1,2] Possible medical and materials applications may be limited by the chemical and physical properties of the natural DNA building blocks. Not surprisingly, the quest for modified building blocks with novel structural and electronic features is increasing.[3–5] The control of the structural organization of the synthetic, functional building blocks still resides in the double helical structure. Thus, DNA serves as a versatile scaffold in the development of different types of materials.[6–16] Previous results from our group showed that an entirely artificial section of twelve or more pyrene 2,8-dicarboxamide units embedded in a double-stranded DNA adopts a helical organization.[17–19] The negatively charged phosphate backbone and the DNA parts guarantee solubility in an aqueous medium of the chimeric oligomers, despite the high lipophilicity of the pyrene residues. In these constructs, the DNA part facilitates the structural organization of the pyrene segments. On the other hand, these amphiphilic oligopyrenotides[20] also have their own, intrinsic structural features and form aggregates *via* directional self-assembly.[21] This observation prompted us to carry out further investigations reducing the DNA part to a minimum, namely one nucleotide pair, to explore if the pyrene units still adopt a defined structure and if transfer of chirality occurs from the nucleotide to the pyrene stacks. Heptapyrenotides (Py_7)[22] assemble into supramolecular polymers.[23–29] Doping with a cytidine modified oligopyrene (Py_7-C) has a significant influence on the optical activity of helical aggregates *via* a mechanism of chiral amplification.[30–32] In general, preferential helicity of columnar stacks can be realized through the introduction of chiral peripheral substituents of the aromatic stacking units or by use of chiral external factors, such as the solvent, ligands or templates.[27,33–47]

In this article we present an extended study of aggregates and co-aggregates of the non-chiral pyrene oligomer (Py_7) and its mono- or di-substituted nucleotide analogs (Py_7-N and N-Py_7-N′). We demonstrate that a single nucleotide may be sufficient for the fine tuning of the aggregates' properties by changing the mechanism of aggregation from isodesmic to nucleation–elongation, which results in amplification of chirality in the supramolecular polymers (Scheme 1).

Results and discussion

To investigate the influence of a single nucleotide on the formation of supramolecular assemblies, oligomers containing seven pyrene units and one or two of the four natural nucleotides were

Department of Chemistry and Biochemistry, University of Bern, Freiestrasse 3, CH-3012 Bern, Switzerland.
E-mail: robert.haener@ioc.unibe.ch; http://haener.dcb.unibe.ch;
Tel: +4131 631 4382

† Dedicated to Professor H. Gobind Khorana.

‡ Electronic supplementary information (ESI) available: Synthetic and analytical details; additional UV/Vis, fluorescence and CD spectra. See DOI: 10.1039/c2ob25320h

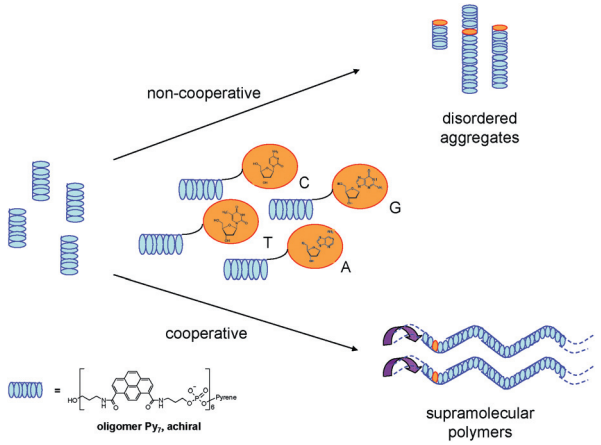

Scheme 1 Influence of single nucleotides on the aggregation of oligomers Py_7 and on amplification of chirality.

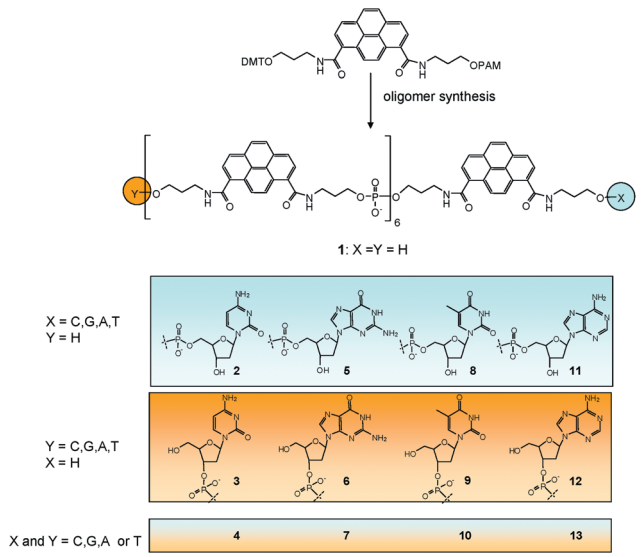

Fig. 1 Oligomers used in the present study. Nucleotides are attached to the oligopyrenotide *via* their 5′- or 3′-ends, *e.g.* **2**, **3**, **4** are cytidine-containing oligomers (for more details see also Table 1).

synthesized (oligomers **1–13**, Fig. 1 and Table 1). The nucleotides were attached either *via* their 5′-oxygen (**2**, **5**, **8**, **11**) or their 3′-oxygen (**3**, **6**, **9**, **12**); oligomers **4**, **7**, **10** and **13** have the same kind of nucleotide attached on each end of the heptapyrenotide.

The oligomers were investigated by absorbance, fluorescence and CD-spectroscopy.[13] Information about the degree of stacking of pyrenes in the oligomers is provided by UV-Vis spectroscopy. Vibronic structures are a result of reduced rotational freedom of the pyrene molecules and are observed if the pyrene molecules are stacked in an ordered way. Fluorescence spectra give an indication about the twisting of the pyrene units within stacks, which appears as a characteristic blue shift of pyrene excimer emission. The most common technique to examine chiral systems is CD-spectroscopy. In the present case, it provides information about the effect of a nucleotide on the formation of non-racemic, chiral pyrene assemblies in contrast to non-chiral aggregates with a random orientation of building blocks, or a racemic mixture of chiral aggregates.

Table 1 Pyrene oligomers used in the study; spectroscopic characteristics of self-aggregates and co-aggregates with oligomer **1**

No.	Oligomer	H%[a]	Aggregation process[b] self/co		CD-type[c] self/co		Remarks[d] self/co	
1	Py_7	43	nucl.	—	—	—		
2	Py_7-C	13	isod.	nucl.	—	2		
3	C-Py_7	23	isod.	nucl.	1	2		
4	C-Py_7-C	16	isod.	nucl.	—	—		
5	Py_7-G	26	isod.	nucl.	—	2^m		
6	G-Py_7	17	isod.	nucl.	2	—	mf	mf
7	G-Py_7-G	17	isod.	nucl.	1	2^m		mf
8	Py_7-T	28	isod.	nucl.	1	—		
9	T-Py_7	14	isod.	nucl.	—	—		
10	T-Py_7-T	12	isod.	nucl.	—	—		
11	Py_7-A	21	isod.	nucl.	—	2^m		
12	A-Py_7	15	isod.	nucl.	1	—	mf	mf
13	A-Py_7-A	12	isod.	isod.	—	—		

[a] At 245 nm upon aggregation; sodium phosphate buffer, pH = 7.0, 1.0 M NaCl; 5 μM total oligomer concentration. [b] Classification of apparent process; self = self-aggregation; co indicates co-aggregation with oligomer **1**; isod. = isodesmic, nucl. = nucleation–elongation. [c] CD-type 1 (see Fig. 3); CD-type 2 (see Fig. 3); CD-type 2^m (mirror image of CD-type 2, see Fig. 3). [d] mf indicates that partial pyrene monomer fluorescence was observed in addition to excimer fluorescence.

Formation of supramolecular polymers upon aggregation of **1** was described recently.[22] Self-association of the oligomers (**2–13**) was studied to elucidate the influence of modification (chiral aromatic molecules) on aggregation/assembly. Association of oligomers with complementary bases **2*6**, **3*5**, **4*7**, **8*12**, **9*11**, **10*13** was tested by mixing the oligomers in a 1 : 1 ratio in analogy to self-assembly of complementary strands in DNA. Moreover, co-aggregation of unmodified **1** with all of its base-modified derivatives **2–13** was investigated. The findings are described below.

Cytidine-modified oligomers (2, 3 and 4)

Fig. 2 shows the normalized absorbance spectra in the range of 300–425 nm for oligomers **1–4** (left) and the co-aggregates **1*2**, **1*3** and **1*4**. Vibronic structures in the absorbance spectra are most pronounced in the case of oligomer **1**, indicating that the stacking interactions between pyrene units are strongest in this oligomer. Co-aggregation of oligomer **1** with oligomers **2–4** shows some degree of vibronic structure. Among them, co-aggregate **1*3** seems to be the most ordered, but less than **1** alone (**1** > **1*3** > **1*2** > **1*4**). In addition to exhibiting the most resolved vibronic structure, oligomer **1** also shows the highest hypochromism upon cooling (Table 1).

The reduction of vibronic structures after addition of one of the nucleotide-modified oligomers indicates a decrease of the fraction of ordered pyrene stacks. Self-aggregation of oligomer **2** shows the smallest hypochromism, meaning that attachment of a 3′-cytidine nucleotide does not support organization within the pyrene stacks.

Temperature-dependent fluorescence spectra show a gradual loss in pyrene excimer emission with increasing temperature

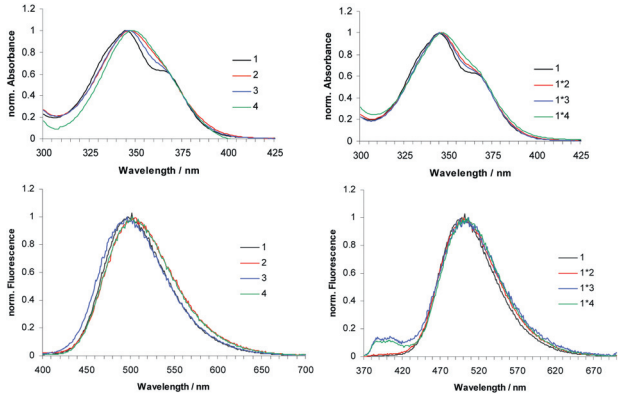

Fig. 2 Normalized absorbance (top) and fluorescence (bottom) spectra; left: oligomers **1** (Py_7), **2** (Py_7-C), **3** (C-Py_7) and **4** (C-Py_7-C); right: co-aggregates of the cytidine-derived oligomers with **1** in a 1 : 1 ratio. Conditions: sodium phosphate buffer, pH = 7.0, 1.0 M NaCl, 20 °C; 5 μM total oligomer concentration.

(ESI, Fig. S18‡) for oligomers **2**–**4**. In Fig. 2 (bottom) the normalized fluorescence spectra of pyrene emission at 20 °C are presented. Self-association of **1** (498 nm) and **3** (497 nm) shows a more pronounced blue shift than **2** (503 nm) and **4** (503 nm) relative to the excimer signals of the co-aggregates **1*2**, **1*3**, **1*4**, which occur at similar wavelength between 503 and 507 nm. Based on the vibronic structures (see above) and the blue shift in pyrene excimer emission, self-aggregates of oligomer C-Py_7 (**3**) seem to be most organized in the cytidine series.

The CD spectrum of oligomer **3** indicates the formation of a chiral structure. A bisignate signal for the pyrene band centred at 340 nm is observed, with a positive Cotton effect at λ = 348 nm, followed by a minimum at λ = 328 nm. At λ = 270 nm, a negative signal appears followed by a more pronounced positive signal at 240 nm. This type of CD-curve will be called CD-type 1, Fig. 3 top. Co-aggregate **1*3** shows a similar CD-effect as described for **1*2**, *i.e.* a bisignate signal for the pyrene band centred at 360 nm with a positive Cotton effect at λ = 373 nm and a negative Cotton effect at λ = 345 nm. Two negative signals were observed at λ = 238 nm and λ = 208 nm (called CD-type 2, Fig. 3 bottom). Co-aggregate **1*3** showed a more intense signal than **1*2**, suggesting that a 5′-cytidine stabilizes the pyrene aggregate better than a 3′-cytidine. Obviously, the site of attachment of the nucleotide plays a role in the formation of aggregates. If the pyrene oligomer is modified with a cytidine on both sides (**4**), no CD-signal is observed (Fig. 3, bottom).

The cooling profiles of self-aggregates of **2**–**4** all fit an isodesmic model (Fig. 4). However, if the oligomers are combined with oligomer **1**, two stages are observed upon decreasing the temperature: formation of a nucleus, followed by an elongation process below 60 °C.[48–52] Thus, co-aggregates **1*2**, **1*3**, **1*4** all exhibit cooperative aggregation behaviour.

Guanosine-modified oligomers (5, 6 and 7)

Apart from oligomer **5**, absorbance spectra of self-aggregates of guanosine-modified oligomers show little or no vibronic

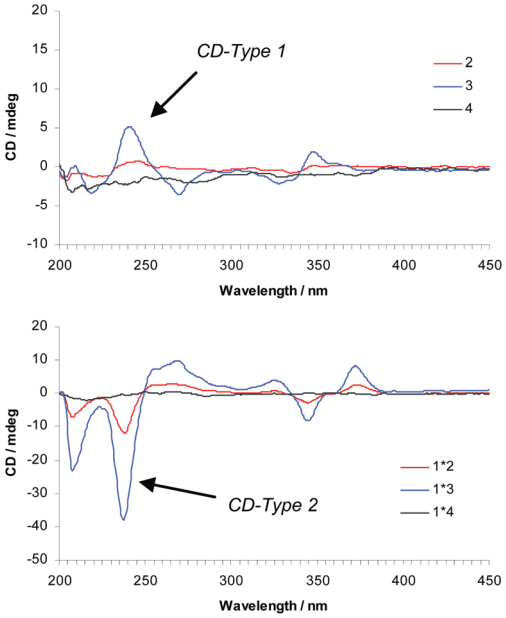

Fig. 3 CD-spectra of cytidine-modified oligomers **2** (Py_7-C), **3** (C-Py_7) and **4** (C-Py_7-C); self-aggregates (top) and co-aggregates with oligomer **1** in a 1 : 1 ratio. Conditions: see Fig. 2.

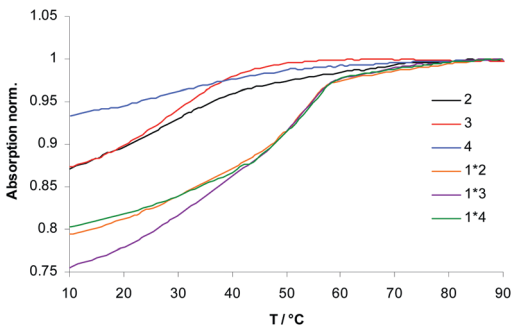

Fig. 4 Cooling profiles of cytidine-modified oligomers **2** (Py_7-C), **3** (C-Py_7) and **4** (C-Py_7-C) alone and as co-aggregates with oligomer **1** in a 1 : 1 ratio. Conditions: 5 μM pyrene oligomer, sodium phosphate buffer, pH = 7.0, 1.0 M NaCl.

structure. The resolution of the vibronic structures observed for the co-aggregates is in the order **1*6** > **1*7** ≈ **1*5** (Fig. 5).

Upon thermal melting, the fluorescence spectra show a gradual reduction of the pyrene excimer emission intensities, except for **7** and co-aggregate **1*6** (ESI, Fig. S19‡). The self-aggregate of oligomer **6** shows, in addition to excimer fluorescence, a considerable pyrene monomer emission (370–420 nm, Fig. 5). A possible explanation could be that the nucleobase guanine, when attached at the 5′-end, can displace one of the pyrene units from the stack, which leads then to an unassociated pyrene and monomer emission. The maxima of the pyrene excimer bands of **5**, **6**, **7**, as well as in their co-aggregates with **1**, are in the narrow range of 503–508 nm.

CD-spectra reveal interesting patterns for the guanosine-modified oligomers. This nucleotide has a positive effect on the chiral organization of the pyrene units if attached to the 5′-end or

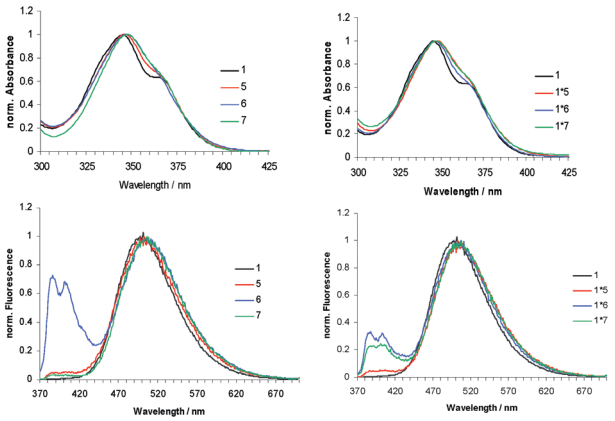

Fig. 5 Normalized absorbance (top) and fluorescence (bottom) spectra; left: oligomers **1** (Py_7), **5** (Py_7-G), **6** (G-Py_7) and **7** (G-Py_7-G); right: co-aggregates of the guanosine-modified oligomers with **1** in a 1 : 1 ratio. Conditions: see Fig. 2.

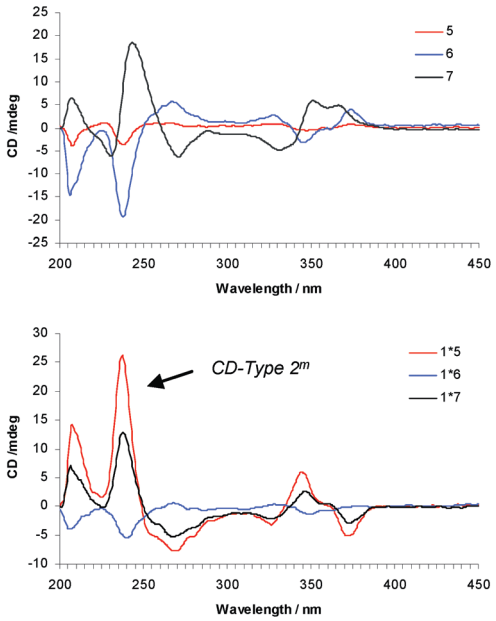

Fig. 6 CD-spectra of guanosine-modified oligomers **5** (Py_7-G), **6** (G-Py_7) and **7** (G-Py_7-G); self-aggregates (top) and co-aggregates with oligomer **1** in a 1 : 1 ratio. Conditions: see Fig. 2.

at both ends of the oligopyrenotide. Apart from oligomer **5** (G attached at the 3′-end) all aggregates are CD-active. Oligomer **6** shows the signal, which was observed for co-aggregates **1*2** and **1*3** (CD-type 2), while oligomer **7** exhibits CD-type 1. Co-aggregate **1*5** shows a quite intense CD with a bisignate signal centered again at 360 nm (negative Cotton effect at λ = 373 nm, positive Cotton effect at λ = 345 nm) and two positive signals at λ = 238 nm and λ = 208 nm. Interestingly, this spectrum (called CD-type 2^m) corresponds to the exact mirror image of the spectrum CD-type 2 described above. This aspect will be discussed later in more detail. Co-aggregate **1*7** shows the same characteristics, though of lesser intensity, and co-aggregate **1*6** showed no defined shape (Fig. 6).

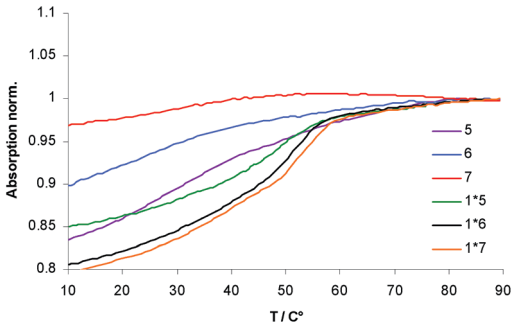

Fig. 7 Cooling profiles of pyrene oligomer modified with guanosine **5** (Py_7-G), **6** (G-Py_7) and **7** (G-Py_7-G), self-aggregates or co-aggregates with oligomer **1** in a 1 : 1 ratio. Conditions: see Fig. 4.

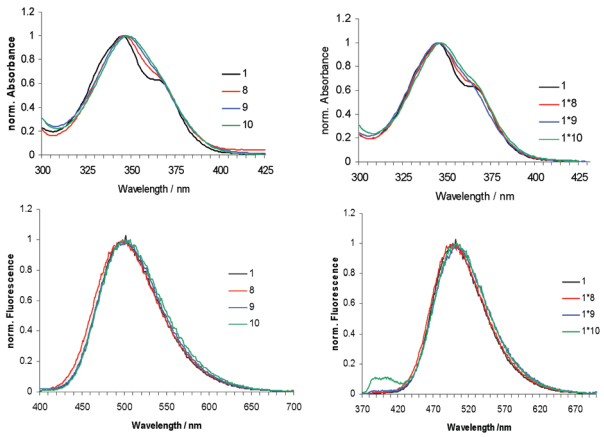

Fig. 8 Normalized absorbance (top) and fluorescence (bottom) spectra; left: oligomers **1** (Py_7), **8** (Py_7-T), **9** (T-Py_7) and **10** (T-Py_7-T); right: co-aggregates of the thymidine-modified oligomers with **1** in a 1 : 1 ratio. Conditions: see Fig. 2.

The cooling profile clearly follows an isodesmic pattern for the self-aggregate of oligomer **7** (Fig. 7). All G-containing co-aggregates with oligomer **1** show a well-defined transition in the range between 50 and 60 °C, indicating the formation of a nucleation/elongation process.

Thymidine-modified oligomers (8, 9 and 10)

Self-association of oligomer **8**, but not of oligomers **9** and **10**, leads to some degree of vibronic structure in absorbance spectra (Fig. 8). Among the co-aggregates, **1*8** exhibits the most pronounced vibronic structure. Pyrene excimer fluorescence is very similar in all self- and co-aggregates of the thymidine-modified oligomers (maxima at 502–507 nm), except for the self-aggregate of oligomer **8**, which is blue shifted (498 nm, see also ESI, Fig. S20‡).

Oligomer **8** shows a strong CD signal (Fig. 9, CD-type 1), whereas oligomers **9** and **10** or their co-aggregates with oligomer **1** showed no distinct Cotton effects. According to the cooling profiles of co-aggregates **1*8** and **1*10** (Fig. 10), assembly-formation follows a nucleation–elongation process, as suggested by the sharp transition points observed at 60 °C (**1*10**) and 47 °C

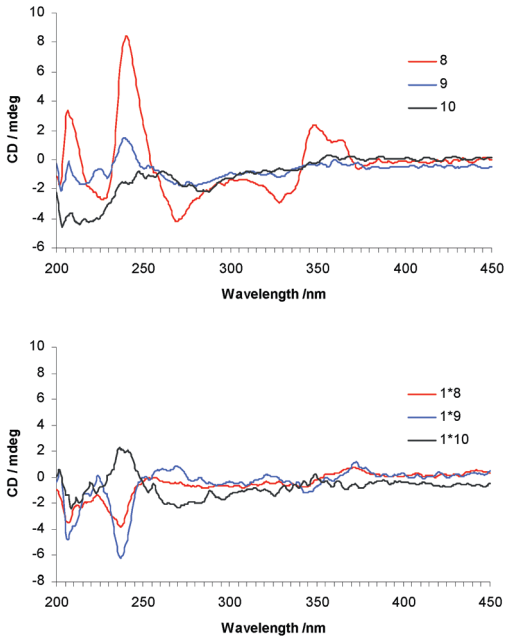

Fig. 9 CD-spectra of pyrene oligomer modified with thymidine **8** (Py_7-T), **9** (T-Py_7) and **10** (T-Py_7-T); self-aggregates (top) and co-aggregates with oligomer **1** in a 1 : 1 ratio. Conditions: see Fig. 2.

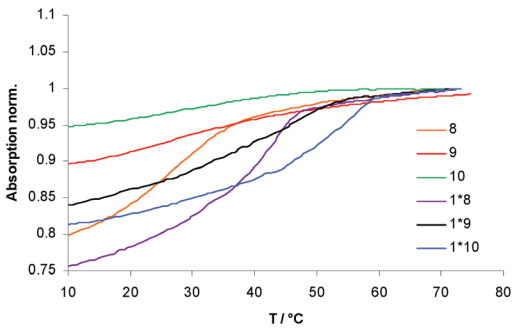

Fig. 10 Cooling profiles of pyrene oligomer modified with thymidine **8** (Py_7-T), **9** (T-Py_7) and **10** (T-Py_7-T), self-aggregates and co-aggregates with oligomer **1** in a 1 : 1 ratio. Conditions: see Fig. 4.

(**1*8**) upon change of temperature.[51] Self-aggregates **8**, **9**, **10** and co-aggregate **1*9** generally follow an isodesmic pattern.

Adenosine-modified oligomers (11, 12 and 13)

The self-aggregates of oligomers **11**, **12** and **13** reveal no pronounced vibronic structures in the UV-Vis spectra. In co-aggregate **1*12** they are more pronounced than in **1*11** or **1*13**. Upon self-association of oligomer **12**, some pyrene monomer emission at 370–420 nm is present (Fig. 11, see also ESI, Fig. S21‡).

CD spectroscopy reveals no distinct signals for self-aggregates **11** and **13** (Fig. 12) and a weak signal for **12**. Co-aggregates **1*12** and **1*13** show no Cotton effects but **1*11** exhibits strong CD signals. Co-aggregation of **1*11** and **1*12** (Fig. 13) proceeds by a nucleation–elongation mechanism. For oligomers **11**, **12** and **13** alone, the assembly/disassembly process follows an isodesmic pattern.

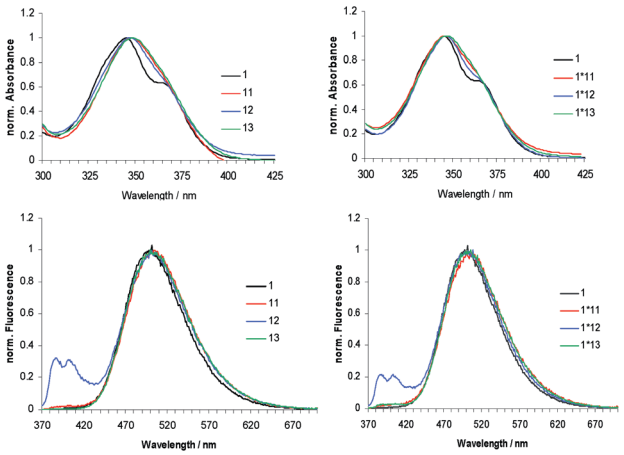

Fig. 11 Normalized absorbance (top) and fluorescence (bottom) spectra; left: oligomers **1** (Py_7), **11** (Py_7-A), **12** (A-Py_7) and **13** (A-Py_7-A); right: co-aggregates of the adenosine-modified oligomers with **1** in a 1 : 1 ratio. Conditions: see Fig. 2.

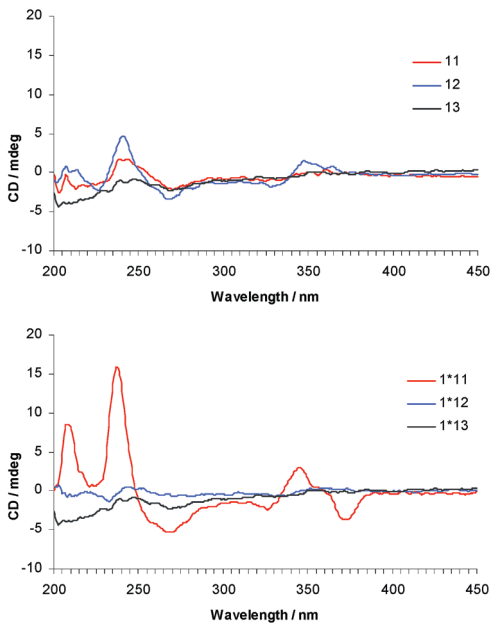

Fig. 12 CD-spectra of pyrene oligomer modified with adenosine **11** (Py_7-A), **12** (A-Py_7) and **13** (A-Py_7-A); self-aggregates (top) and co-aggregates with oligomer **1** in a 1 : 1 ratio. Conditions: see Fig. 2.

Supramolecular polymers

Supramolecular polymers are dynamic, polymeric aggregates of monomeric units, held together by reversible and directional, non-covalent interactions.[24,53–56] The lengths of the chains are related to the strength of the non-covalent interactions and the concentration of the monomers.[57] Furthermore, the reversibility of non-covalent bond formation ensures the self-healing of initially formed defective sites during polymer assembly under equilibrium conditions. The self-assembly process can be described by two main models. In an isodesmic process, the assembly is non-cooperative and the association is identical at any step of the polymerization process, which is characterized by

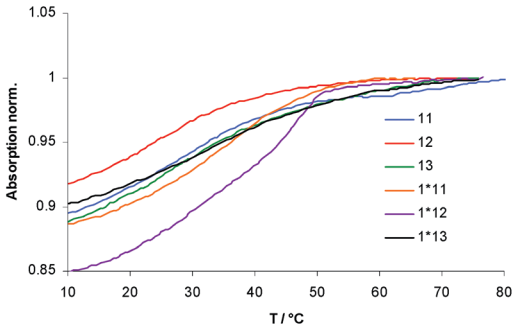

Fig. 13 Cooling profiles of pyrene oligomer modified with adenosine **11** (Py_7-A), **12** (A-Py_7) and **13** (A-Py_7-A), self-aggregates and co-aggregates with oligomer **1** in a 1 : 1 ratio. Conditions: see Fig. 4.

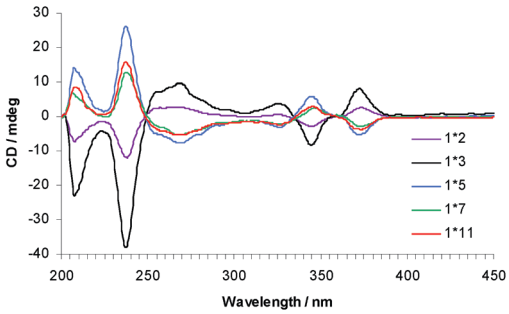

Fig. 14 CD-spectra of co-aggregates between pyrene oligomers **2** (Py_7-C), **3** (C-Py_7), **5** (Py_7-G), **7** (G-Py_7-G) and **11** (Py_7-A) with oligomer **1** in a 1 : 1 ratio; note the mirror-inverted shape of the curves. Conditions: see Fig. 2.

a single binding constant.[49] The characteristics of a nucleated mechanism are a rather slow pre-aggregation of a certain number of building blocks forming a nucleus (nucleation), which is then followed by a rapid process of chain propagation.[50] The latter mechanism usually takes place in the growth of ordered supramolecular polymers.[57] By changing external parameters, *e.g.* the temperature, information may be obtained on the mechanism by which the self-assembly proceeds.

It was found previously that supramolecular polymerization of oligomer **1** occurs *via* a nucleated process.[22] The data presented here extend these preliminary studies and show that the self-association of all nucleotide-modified pyrene oligomers **2–13** follows an isodesmic model. In the formation of co-aggregates with oligomer **1**, however, significant differences are observed. All co-aggregations with oligomers modified by the nucleotides cytidine (**1*2**, **1*3**, **1*4**) and guanosine (**1*5**, **1*6**, **1*7**) proceed in a nucleated self-assembly process. Also, for the co-aggregates **1*8** (with Py_7-T) and **1*10** (with T-Py_7-T) the formation of a nucleus is observed. In the adenosine series, a nucleation process is not observed for **1*13** (A-Py_7-A), but when adenosine is attached at only one of the two sides (**1*11** and **1*12**) formation of a nucleus is observed. Thus, it can be concluded that, even though the modified oligomers interact among themselves in a non-cooperative way, they form supramolecular polymers in combination with the heptapyrenotide Py_7 (**1**). The interaction, however, is dependent on the nature and position of the attached nucleotide. While some of the described oligomers completely prevent the formation of a nucleus (oligomers **9** T-Py_7 and **13** A-Py_7-A), most of them proceed *via* a nucleation process in the co-aggregation with oligomer **1**.

Helical chirality of supramolecular polymers

Helical chirality originates from the unidirectional twist of building blocks along the propagation axis.[58] Natural helical polymers, such as DNA and proteins, are composed of enantiomerically pure, chiral building blocks. The adopted helical sense corresponds, thus, to the thermodynamically favored diastereomer. The heptapyrenotide **1**, however, is achiral. Consequently, its folding into a helical conformation will lead to a racemic mixture of right- and left-handed helices in the absence of external, symmetry breaking factors. The presence of a chiral inductor, however, may lead to the preferential formation of one type of helix.[43,59] In the present case, the chiral inductor is a heptapyrenotide bearing one or two terminally attached nucleotides (C, G, T or A, oligomers **2–13**). Oligomer **1** forms supramolecular polymers under conditions of high ionic strength in aqueous medium. The polymerization process proceeds through a nucleation step. The effect of copolymerization with all of the chiral oligomers **2–13** was systematically investigated. Most of the co-aggregates were found to form supramolecular polymers. The attached nucleotides, however, are not in all cases able to shift the equilibrium towards one of the two enantiomeric helices, as evidenced by the absence of a CD-signal. CD-inactive co-aggregates were observed with oligomers **4** (C-Py_7-C), **6** (G-Py_7), **8** (Py_7-T), **10** (T-Py_7-T) and **12** (A-Py_7; Fig. 3, 6, 9 and 12).

Oligomers **2** (Py_7-C), **3** (C-Py_7), **5** (Py_7-G), **7** (G-Py_7-G) and **11** (Py_7-A) are most suitable to shift the equilibrium in either direction. The formation of the assemblies occurs *via* supramolecular polymerization (see Fig. 4, 7, 10 and 13) and the appearance of a characteristic CD signal is observed. All CD curves are shown in combination in Fig. 14. The shapes correspond to CD-type 2 or its mirror image CD-type-2^m. Oligomers **2**, **3**, **5**, **7**, and **11** are modified with nucleotides cytidine, guanosine or adenosine. Depending on the nucleotide the helical sense of the polymers can be shifted towards either form, *i.e.* **5**, **7** and **11** induce the *M*-helix, **2** and **3** the *P*-helix. Thymidine seems not suitable to favor one enantiomer of the supramolecular polymers.

Self-aggregates of **3**, **7**, **8** and **12** show a third type of signal (CD-type 1). The fact that the cooling follows an isodesmic pattern strongly suggests that smaller complexes are formed rather than supramolecular polymers by these oligomers. The nature of these complexes is still under investigation.

Amplification of chirality

Amplification of chirality was first described in the pioneering work by Green and coworkers studying polyisocyanates.[30,31] This phenomenon is not limited to covalently linked polymers but occurs also in non-covalent supramolecular assemblies.[27] Minute amounts of a chiral seed compound may be sufficient to render the polymers homochiral.[22,32] The fact that some of the oligomers showed very intense Cotton effects in the co-aggregates with **1** prompted us to study the amplification of the

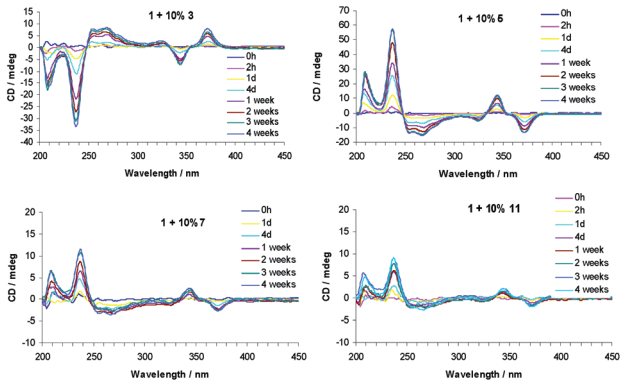

Fig. 15 Amplification of chirality; oligomer **1** with 10% of oligomers **3** (C-Py_7), **5** (Py_7-G), **7** (G-Py_7-G) and **11** (Py_7-A). Conditions: see Fig. 1.

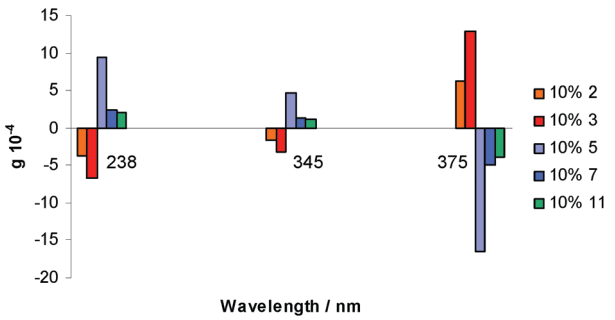

Fig. 16 *g*-Factor; oligomer **1** with 10% of oligomers **2** (Py_7-C), **3** (C-Py_7), **5** (Py_7-G), **7** (G-Py_7-G) or **11** (Py_7-A). Conditions: see Fig. 1.

chirality effect, using 10% of the corresponding chiral oligomer (Fig. 15). The development of the signals was monitored over a period of 4 weeks. Growth of the CD signals, and thus amplification of chirality, was observed with oligomers **3**, **5**, **7** and **11**.

In Fig. 16, the calculated *g*-factors are shown for the 9 : 1 ratio of oligomer **1** with either oligomer **2**, **3**, **5**, **7** or **11** (corresponding to a 70 : 1 pyrene–nucleobase ratio). Guanosine attached at the 3′-end has the highest impact on the amplification of chirality. The pyrene oligomers are highly sensitive to the chiral nature of the nucleoside guanosine. Further it could be shown that in the case of the nucleotide cytidine the point of attachment has a remarkable impact on the *g*-factor: the amplification of chirality is much more pronounced if the nucleotide is located at the 5′-end (**3**) rather than at the 3′-end (**2**).

The effect of Watson–Crick complementarity

Association of oligomers with complementary nucleobases **2*6**, **3*5**, **4*7**, **8*12**, **9*11**, **10*13** was tested by mixing the oligomers in a 1 : 1 ratio in analogy to the self-assembly of complementary strands in DNA. Fluorescence and CD-spectra (ESI, Fig. S24–S27‡) allow no clear conclusions regarding the interactions between the nucleobases of two types of oligomers in the corresponding mixtures. Most likely, mixtures of self- and mixed aggregates are formed in these cases. This is supported by the observation that the mixtures show partially the same characteristics as the corresponding self-aggregates, but to a smaller degree. All melting profiles of the aggregates **2*6**, **3*5**, **4*7**, **8*12** and **10*13** indicate no formation of extended supramolecular polymers (ESI, Fig. S28‡).

Conclusions

Formation of supramolecular polymers *via* aggregation of oligomer **1** was recently communicated. An extended study of self- and co-aggregation of the achiral heptapyrenotide Py_7 (**1**) and its nucleotide-modified derivatives Py_7-N and N-Py_7-N (**2–13**) was conducted to investigate the influence of the chiral modification on the polymerization behaviour. Self-association of the nucleotide-modified oligomers **2–13** was shown in all cases to follow an isodesmic model; the formation of long assemblies is absent. Co-aggregation of **1** with the large majority of nucleotide-modified oligomers follows a nucleation–elongation process, which is characteristic of the formation of supramolecular polymers.

The supramolecular polymers formed by aggregation of **1** are present as a racemic mixture of helical aggregates. A single nucleotide present in oligomers **2–13** can favor one of the two enantiomeric helices in co-aggregates with oligomer **1**. Oligomers **2** (Py_7-C), **3** (C-Py_7), **5** (Py_7-G), **7** (G-Py_7-G) and **11** (Py_7-A) induce preferential formation of one of the enantiomers. Amplification of chirality could be observed in the presence of 10% of these oligomers. Aggregates of oligomers with complementary nucleotides (**2*6**, **3*5**, **4*7**, **8*12** and **10*13**) show no signs of supramolecular polymerization.

The data demonstrate that the formation of supramolecular polymers from oligopyrenotides is very sensitive to the nature of chiral auxiliaries. Supramolecular polymerization follows a nucleation–elongation mechanism and leads to amplification of chirality. Oligopyrenotides are, thus, valuable oligomeric building blocks for the generation of optically active polymeric materials.

Acknowledgements

Financial support by the Swiss National Foundation (grant 200020-132581) is gratefully acknowledged.

Notes and references

1 N. C. Seeman, *Acc. Chem. Res.*, 1997, **30**, 357–363.
2 C. A. Mirkin, R. L. Letsinger, R. C. Mucic and J. J. Storhoff, *Nature*, 1996, **382**, 607–609.
3 E. T. Kool, *Chem. Rev.*, 1997, **97**, 1473–1487.
4 J. Wengel, *Acc. Chem. Res.*, 1999, **32**, 301–310.
5 F. D. Lewis, R. L. Letsinger and M. R. Wasielewski, *Acc. Chem. Res.*, 2001, **34**, 159–170.
6 N. C. Seeman, *Annu. Rev. Biochem.*, 2010, **79**, 65–87.
7 C. K. McLaughlin, G. D. Hamblin and H. F. Sleiman, *Chem. Soc. Rev.*, 2011, **40**, 5647–5656.
8 K. Kinbara and T. Aida, *Chem. Rev.*, 2005, **105**, 1377–1400.
9 F. A. Aldaye, A. L. Palmer and H. F. Sleiman, *Science*, 2008, **321**, 1795–1799.
10 T. Torring, N. V. Voigt, J. Nangreave, H. Yan and K. V. Gothelf, *Chem. Soc. Rev.*, 2011, **40**, 5636–5646.
11 U. Feldkamp and C. M. Niemeyer, *Angew. Chem., Int. Ed.*, 2006, **45**, 1856–1876.
12 M. Endo and H. Sugiyama, *ChemBioChem*, 2009, **10**, 2420–2443.

13 V. L. Malinovskii, D. Wenger and R. Häner, *Chem. Soc. Rev.*, 2010, **39**, 410–422.
14 A. Ruiz-Carretero, P. G. A. Janssen, A. Kaeser and A. P. H. J. Schenning, *Chem. Commun.*, 2011, **47**, 4340–4347.
15 A. Mammana, G. Pescitelli, T. Asakawa, S. Jockusch, A. G. Petrovic, R. R. Monaco, R. Purrello, N. J. Turro, K. Nakanishi, G. A. Ellestad, M. Balaz and N. Berova, *Chem.–Eur. J.*, 2009, **15**, 11853–11866.
16 P. P. Neelakandan, Z. Pan, M. Hariharan, Y. Zheng, H. Weissman, B. Rybtchinski and F. D. Lewis, *J. Am. Chem. Soc.*, 2010, **132**, 15808–15813.
17 V. L. Malinovskii, F. Samain and R. Häner, *Angew. Chem., Int. Ed.*, 2007, **46**, 4464–4467.
18 V. A. Galievsky, V. L. Malinovskii, A. S. Stasheuski, F. Samain, K. A. Zachariasse, R. Häner and V. S. Chirvony, *Photochem. Photobiol. Sci.*, 2009, **8**, 1448–1454.
19 F. Samain, V. L. Malinovskii, S. M. Langenegger and R. Häner, *Bioorg. Med. Chem.*, 2008, **16**, 27–33.
20 R. Häner, F. Garo, D. Wenger and V. L. Malinovskii, *J. Am. Chem. Soc.*, 2010, **132**, 7466–7471.
21 R. Häner, F. Samain and V. L. Malinovskii, *Chem.–Eur. J.*, 2009, **15**, 5701–5708.
22 A. L. Nussbaumer, D. Studer, V. L. Malinovskii and R. Häner, *Angew. Chem., Int. Ed.*, 2011, **50**, 5490–5494.
23 J. S. Moore, *Curr. Opin. Colloid Interface Sci.*, 1999, **4**, 108–116.
24 L. Brunsveld, B. J. B. Folmer, E. W. Meijer and R. P. Sijbesma, *Chem. Rev.*, 2001, **101**, 4071–4097.
25 J. M. LEHN, *Polym. Int.*, 2002, **51**, 825–839.
26 T. F. A. de Greef, M. M. J. Smulders, M. Wolffs, A. P. H. J. Schenning, R. P. Sijbesma and E. W. Meijer, *Chem. Rev.*, 2009, **109**, 5687–5754.
27 K. Maeda and E. Yashima, *Top. Curr. Chem.*, 2006, **265**, 47–88.
28 L. C. Palmer and S. I. Stupp, *Acc. Chem. Res.*, 2008, **41**, 1674–1684.
29 J. D. Hartgerink, E. R. Zubarev and S. I. Stupp, *Curr. Opin. Solid State Mater. Sci.*, 2001, **5**, 355–361.
30 M. M. Green, N. C. Peterson, T. Sato, A. Teramoto, R. Cook and S. Lifson, *Science*, 1995, **268**, 1860–1866.
31 M. M. Green, M. P. Reidy, R. J. Johnson, G. Darling, D. J. Oleary and G. Willson, *J. Am. Chem. Soc.*, 1989, **111**, 6452–6454.
32 A. R. A. Palmans and E. W. Meijer, *Angew. Chem., Int. Ed.*, 2007, **46**, 8948–8968.
33 M. M. Green, in *Circular Dichroism – Principles and Applications*, ed. N. Berova, K. Nakanishi and R. W. Woody, Wiley-VCH, Hoboken, NJ, 2000, pp. 491–520.
34 H. Engelkamp, S. Middelbeek and R. J. M. Nolte, *Science*, 1999, **284**, 785–788.
35 M. M. J. Smulders, A. P. H. J. Schenning and E. W. Meijer, *J. Am. Chem. Soc.*, 2008, **130**, 606–611.
36 A. J. Markvoort, H. M. M. ten Eikelder, P. A. J. Hilbers, T. F. A. de Greef and E. W. Meijer, *Nat. Commun.*, 2011, **2**, 509.
37 A. Lohr and F. Wurthner, *Angew. Chem., Int. Ed.*, 2008, **47**, 1232–1236.
38 F. Garcia and L. Sanchez, *J. Am. Chem. Soc.*, 2011, **134**, 734–742.
39 A. Lohr and F. Würthner, *Isr. J. Chem.*, 2011, **51**, 1052–1066.
40 B. L. Feringa and R. A. van Delden, *Angew. Chem., Int. Ed.*, 1999, **38**, 3418–3438.
41 S. J. George, Z. Tomovic, M. M. J. Smulders, T. F. A. de Greef, P. E. L. G. Leclere, E. W. Meijer and A. P. H. J. Schenning, *Angew. Chem., Int. Ed.*, 2007, **46**, 8206–8211.
42 D. Monti, M. Venanzi, G. Mancini, C. D. Natale and R. Paolesse, *Chem. Commun.*, 2005, 2471–2473.
43 E. Yashima, K. Maeda, H. Iida, Y. Furusho and K. Nagai, *Chem. Rev.*, 2009, **109**, 6102–6211.
44 K. Morino, N. Watase, K. Maeda and E. Yashima, *Chem.–Eur. J.*, 2004, **10**, 4703–4707.
45 B. Isare, M. Linares, L. Zargarian, S. Fermandjian, M. Miura, S. Motohashi, N. Vanthuyne, R. Lazzaroni and L. Bouteiller, *Chem.–Eur. J.*, 2010, **16**, 173–177.
46 D. Pijper and B. L. Feringa, *Soft Matter*, 2008, **4**, 1349–1372.
47 M. Albrecht, *Angew. Chem., Int. Ed.*, 2005, **44**, 6448–6451.
48 F. Oosawa and M. Kasai, *J. Mol. Biol.*, 1962, **4**, 10–21.
49 R. B. Martin, *Chem. Rev.*, 1996, **96**, 3043–3064.
50 D. H. Zhao and J. S. Moore, *Org. Biomol. Chem.*, 2003, **1**, 3471–3491.
51 M. M. J. Smulders, M. M. L. Nieuwenhuizen, T. F. A. de Greef, P. van der Schoot, A. P. H. J. Schenning and E. W. Meijer, *Chem.–Eur. J.*, 2010, **16**, 362–367.
52 T. E. Kaiser, V. Stepanenko and F. Würthner, *J. Am. Chem. Soc.*, 2009, **131**, 6719–6732.
53 A. W. Bosman, R. P. Sijbesma and E. W. Meijer, *Mater. Today*, 2004, **7**, 34–39.
54 J. M. Lehn, *Prog. Polym. Sci.*, 2005, **30**, 814–831.
55 G. M. Whitesides, J. P. Mathias and C. T. Seto, *Science*, 1991, **254**, 1312–1319.
56 J. S. Lindsey, *New J. Chem.*, 1991, **15**, 153–180.
57 T. F. A. Greef and E. W. Meijer, *Nature*, 2008, **453**, 171–173.
58 G. A. Hembury, V. V. Borovkov and Y. Inoue, *Chem. Rev.*, 2008, **108**, 1–73.
59 E. Yashima, *Nat. Chem.*, 2011, **3**, 12–14.

